

A Frequency Standard for Today's WWVB

The author shares the design of his frequency standard that's fully compatible with today's WWVB.

For over a half century, the 60 kHz carrier from WWVB has served as a popular and highly respected frequency reference among many scientific, research, and engineering professionals across North America. As GPS-disciplined frequency standards started gaining in popularity, the use of WWVB in frequency reference applications began to decline. With this decline, however, came a tremendous increase in the sale and application of low-cost radio controlled "atomic clocks" that receive time and date information from WWVB on a regular basis. This drastic shift in the use of WWVB by the American public forced a realignment of the priorities set for the station by the National Institute of Standards and Technology (NIST).

With the rapid proliferation of radio-controlled clocks came a realization that reception of the WWVB time code by low-cost consumer products was often unreliable. In the eastern United States where signals from the Fort Collins, Colorado WWVB transmitter are often the weakest, competition from high noise levels and co-channel interference from British radio station MSF made reception especially difficult. Enhancements were made to the WWVB effective radiated power and modulation depth, but reception difficulties continued to persist. Finally, when attempts to commission a second WWVB transmitter to serve the east coast failed to reach fruition by the end of 2009, thoughts turned toward making more aggressive changes to WWVB broadcasts that would help improve reception reliability while maintaining compatibility with the millions of radio-controlled clocks already in operation.



— Certificate of Participation —

ARRL Centennial – W1ØØAW/5

April 2014 Frequency Measuring Test

April 10, 2014

This certifies that

John A. Magliacane, KD2BD

submitted frequency measurements taken during the April 2014 Frequency Measuring Test.

The results are as follows:

Band	Measured Frequency (Hz)	Frequency Error (Hz)	Error (± Parts Per Million)
80m	3,598,137.75	0.01	<0.01
40m	7,058,632.38	0.01	<0.01

W1ØØAW/5 Transmit Frequencies
80 meters – 3,598,137.74 Hz
40 meters – 7,058,632.37 Hz
20 meters – 14,121,135.32 Hz


 W1AW Station Trustee

Figure 1 — The author's very successful Frequency Measuring Test results are achieved by using WWVB as a precision frequency reference.

New Modulation Format

NIST realized that only through a radical change in time code transmission and greater sophistication in receiving techniques would any further improvement in reception reliability be achieved. They decided to add a new time code to the WWVB carrier, modulated by means of binary phase

shift keying (BPSK), that next generation radio-controlled clocks could be designed to receive and process with improved reliability. While over-the-air tests conducted in 2012 revealed that the addition of the new BPSK time code had little or no effect on the operation of existing radio-controlled clocks, it

caused every WWVB-disciplined frequency standard to lose phase reference with the WWVB carrier, and thus malfunction. With GPS-based frequency standards in wide use and rising steadily in popularity, and commercial WWVB-based frequency standards out of production for years, NIST decided to permanently add its new BPSK time code to WWVB broadcasts beginning on October 29, 2012, and force all previously functioning WWVB-disciplined frequency standards into obsolescence.

Despite this WWVB priority shift toward

application in consumer products, and away from the scientific and engineering communities, the WWVB carrier frequency is maintained to within one part in 10^{14} , and continues to be derived from a set of four cesium clocks.¹ As such, provided that BPSK compatible reception techniques are employed, radio station WWVB can continue to serve as a reliable and accurate frequency reference, and can do so with a level of precision that far exceeds that of its time dissemination.

A BPSK-Compatible Frequency Standard

The frequency standard described here employs a combination of linear signal processing, vector demodulation, and super-heterodyne receiving techniques to not only discipline a 10 MHz voltage-controlled, temperature-compensated crystal oscillator (VCTCXO) against the WWVB carrier, but also decode its amplitude modulated time code. A wide variety of calibration signals are available to the user, while an LCD display provides NIST (UTC) date, time, and UT1 offset information. Several audio outputs are provided to help assess reception quality and assist in selecting an optimum antenna placement and orientation. An RS-232 port is also included to provide UTC time and date information to external devices.

Performance

The stability and accuracy of a frequency standard are difficult to assess and quantify without making a direct comparison against another standard of superior precision. Even while lacking a second standard, however, some conclusions can be drawn based on the performance a frequency standard demonstrates while being employed in critical applications over the course of many years. For example, the results achieved while employing this frequency standard during Frequency Measuring Tests over the past decade have consistently equaled or surpassed those of most other participants, many of whom employ advanced digital signal processing techniques, commercial GPS-disciplined frequency standards, rubidium oscillators, and other laboratory grade

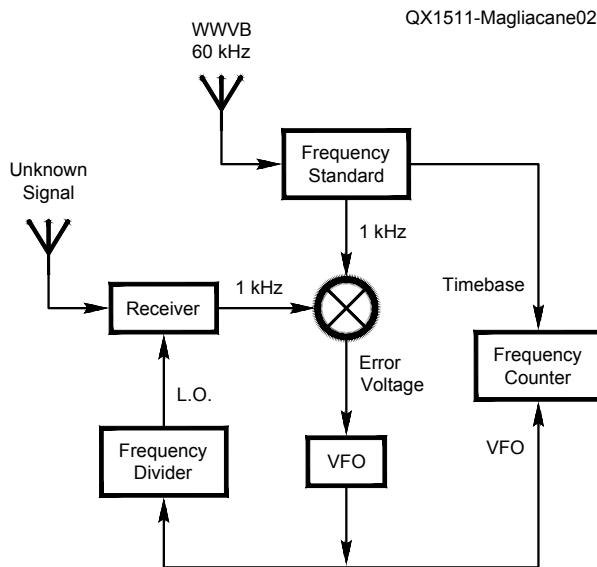


Figure 2 — The author's FMT methodology applies a DC tuning voltage to the local oscillator of a direct conversion receiver to lock its audio output in phase with that of a 1 kHz reference. The frequency of the unknown signal is determined by measuring the frequency of the LO and factoring in the 1 kHz tuning offset.

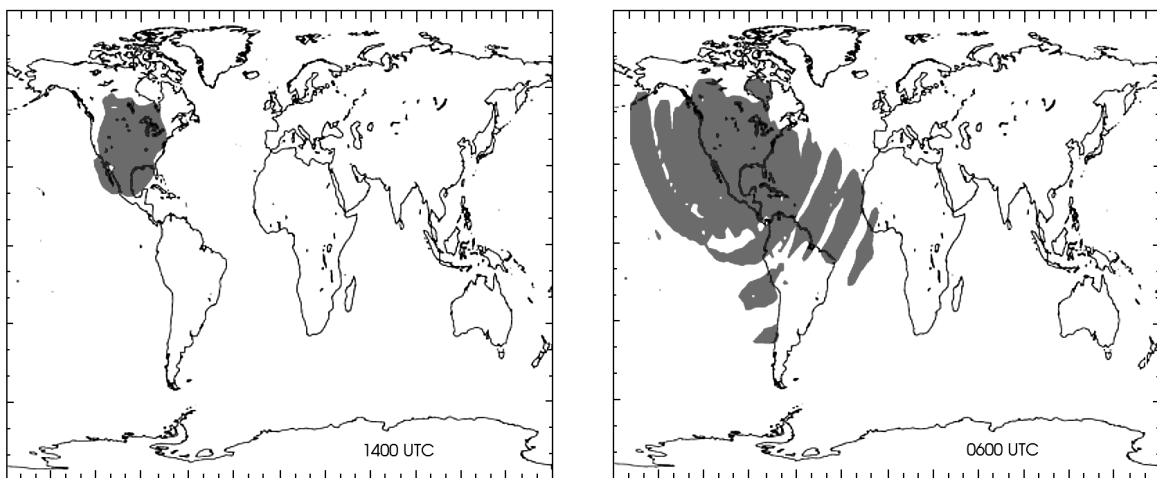


Figure 3 — Space and Naval Warfare Systems (SPAWAR) Command computer simulations illustrate how the WWVB $100 \mu\text{V}/\text{m}$ signal level contours contract during the day and expand during nighttime hours. (Images from NIST website.)

instrumentation. Figure 1 shows a certificate I received for my participation in the April 2014 FMT.

Since the influence of ionospheric perturbations and inaccuracies in frequency measurement methodologies are often the largest consistent sources of error in FMTs, these results alone cannot speak to the full performance of this frequency standard. Using the identical hardware and methodology as those employed in FMTs (Figure 2), I measured the carrier frequencies of many AM broadcast stations received over ground wave paths to a resolution of 312.5 microhertz (less than one part per billion at 1 MHz). During the process, several transmitters were identified as consistently having no measurable frequency error, some of which are known to employ GPS-disciplined rubidium frequency standards for carrier generation. I believe that transmitters exhibiting very small but measurable frequency offsets were likely rubidium controlled but not necessarily GPS-locked, while others that exhibited larger errors that varied over time might have simply been crystal controlled.

Since the GPS-disciplined radio station carriers stood out so clearly among all other stations measured, it follows that the accuracy and stability of this frequency standard probably exceeds the resolution of the measurements taken. In fact, they are possibly several orders of magnitude better based on the known precision to which the WWVB carrier frequency is maintained, and the recognized RF propagation characteristics that exist at low frequencies.

60 kHz Propagation

LF radio propagation is substantially different from that which exists at higher frequencies. Its remarkable stability and reliability have often led to the belief that 60 kHz signals propagate great distances over ground wave paths alone. In reality, a combination of surface wave and D-layer ionospheric paths are responsible for WWVB signal propagation. At night, cosmic background radiation supports a level of D-layer ionization that is sufficient for propagating LF (and lower frequency) radio signals over long distances.² Greater D-layer efficiencies and increased effective height with decreased ionization levels contribute to greater signal coverage during the nighttime hours. See Figure 3.

Diurnal shifts in the height of the D-layer cause changes in the RF path length between WWVB and receivers to occur during the time the RF path undergoes sunrise and sunset transitions. While the accompanying Doppler shifts during these periods are generally small, their effects are cyclic and predictable, and can be handled using a priori knowledge. Long-term frequency accura-

cies very closely approaching those of the WWVB transmitted carrier frequency can be achieved by integrating the diurnal perturbations over a day or more.

WWVB Signal Characteristics

With rare exception, WWVB broadcasts 24 hours a day with a peak envelope effective radiated power of 70 kW. The beginning of every UTC second is identified by a 17 dB reduction in radiated power. See Figure 4. If

the carrier amplitude is restored to full power 200 ms later, this represents a “0” bit in the WWVB legacy time code. If it is restored 500 ms later, this represents a “1” bit in the WWVB time code. If it is restored 800 ms later, this represents a “Marker” bit, one of which is sent every 10 seconds to establish frame synchronization in receivers. Two Marker bits transmitted in succession identify the beginning of a new time code frame and the start of a new UTC minute. Over the course of one minute, the individual “1”s and

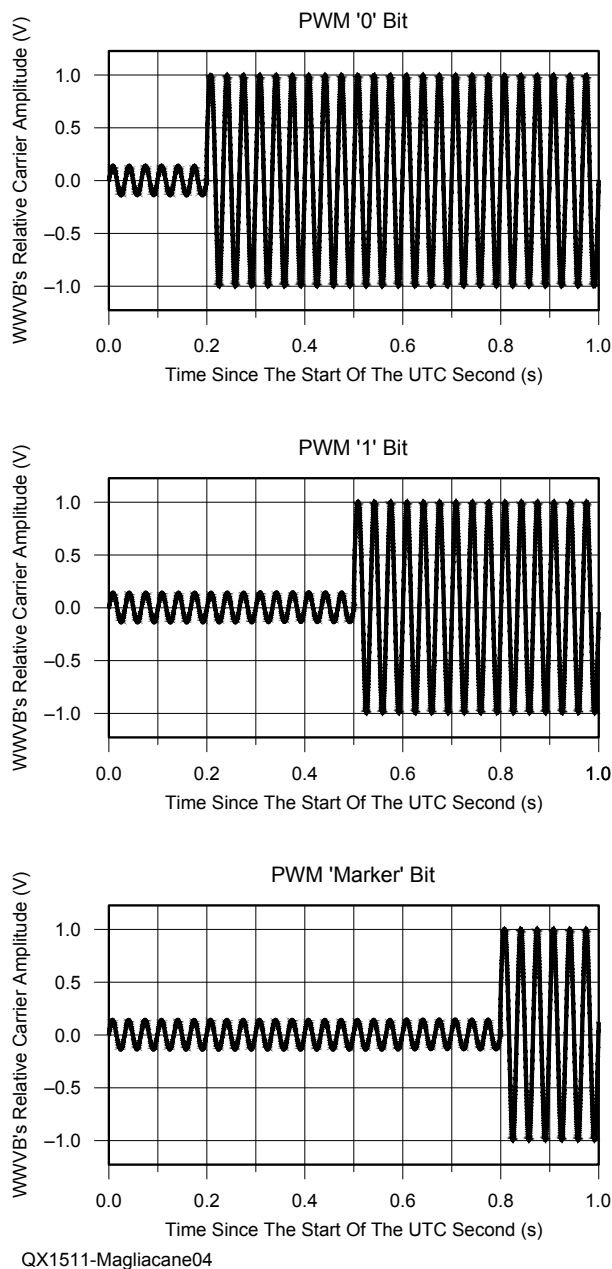


Figure 4 — The WWVB carrier is reduced in amplitude by 17 dB at the beginning of every second. If full power is restored 200 ms later, this represents a “0” bit. If restoration occurs 500 ms later, this represents a “1” bit. If it is restored 800 ms later, this represents a “Marker” bit. The new WWVB BPSK time code is not shown in this illustration.

“0”s produce a pattern that conveys the current date and time, UT1 offset, leap second, and daylight savings time information.

WWVB recently added a secondary time code in the form of BPSK, which co-exists independent of the original amplitude modulated time code. If the phase of the WWVB carrier is reversed 100 ms after the beginning of the UTC second, this represents a “1” bit in the BPSK time code. If no carrier phase reversal takes place at this time, it represents a “0” bit.

The new BPSK time code offers enhanced performance through error detection and correction algorithms, as well as several different modes of operation, not all of which have been fully implemented at this time. While the frequency standard described here possesses BPSK demodulation capability, it is employed solely for the detection and removal of BPSK prior to the carrier phase tracking circuitry that follows.

A Low-Noise WWVB Antenna

Unlike GPS, WWVB reception does not require the use of an outdoor antenna, nor does it require a clear view of the sky. Low-cost consumer grade radio controlled clocks employ electrically small H-Field ferrite loopstick antennas that operate on the same principle as those found in portable AM broadcast band radios. Significantly higher signal levels and noticeably less sensitivity to nearby structures can be realized by using physically larger air-core loop antennas.

While it can take a lot of wire and a lot of labor to wind a 60 kHz resonant air-core loop antenna, just a single turn of multi-conductor ribbon cable can produce an effective multi-turn loop provided that each conductor is

connected in series with its adjacent conductor to form a continuous coil. See Figure 5 for an example of how such a coil can be wired. I fabricated an antenna from a 5 meter length of 40 conductor #28 AWG stranded ribbon cable, and supported it from the ceiling of my attic. Figure 6 shows my antenna installation.

Resonance is achieved by introducing an appropriate amount of capacitance in parallel with the loop. Aligning the plane of the loop in the direction of Fort Collins, Colorado allows the WWVB horizontally polarized H-Field to cut through the center of the loop and induce a voltage across its terminals. Along the eastern edge of the 100 μV /

meter signal contour in central New Jersey, WWVB typically induces several millivolts (peak-to-peak) of RF across the 40 turn loop.

Antenna Preamplifier

A preamplifier located immediately adjacent to the loop provides an important interface between the high-impedance balanced loop antenna and the unbalanced, ground-referenced circuitry that follows. Figure 7 shows the schematic diagram of the preamplifier. The preamplifier connects to the frequency standard through a length of coaxial cable, and it receives its operating

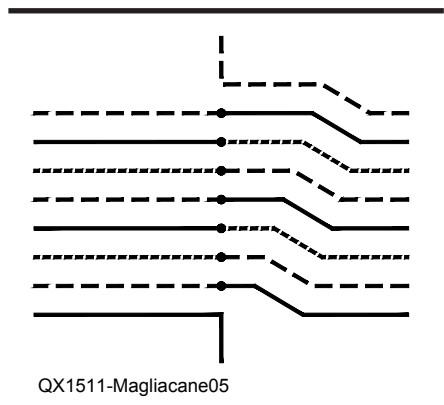


Figure 5 — Loop antenna construction. The ends of the multi-conductor cable are brought together at the bottom of the loop to form a multi-turn coil. After going around once, the end of conductor #1 connects to the beginning of conductor #2, conductor #2 connects to conductor #3, and so on. The uncommitted ends of the first and last conductors form the ends of the coil.



Figure 6 — The author's attic-mounted loop antenna. With the plane of the loop aligned toward Fort Collins, Colorado, the WWVB horizontally polarized H-Field cuts through the center of the loop and induces a voltage across it. The frequency standard amplifies and processes this signal.

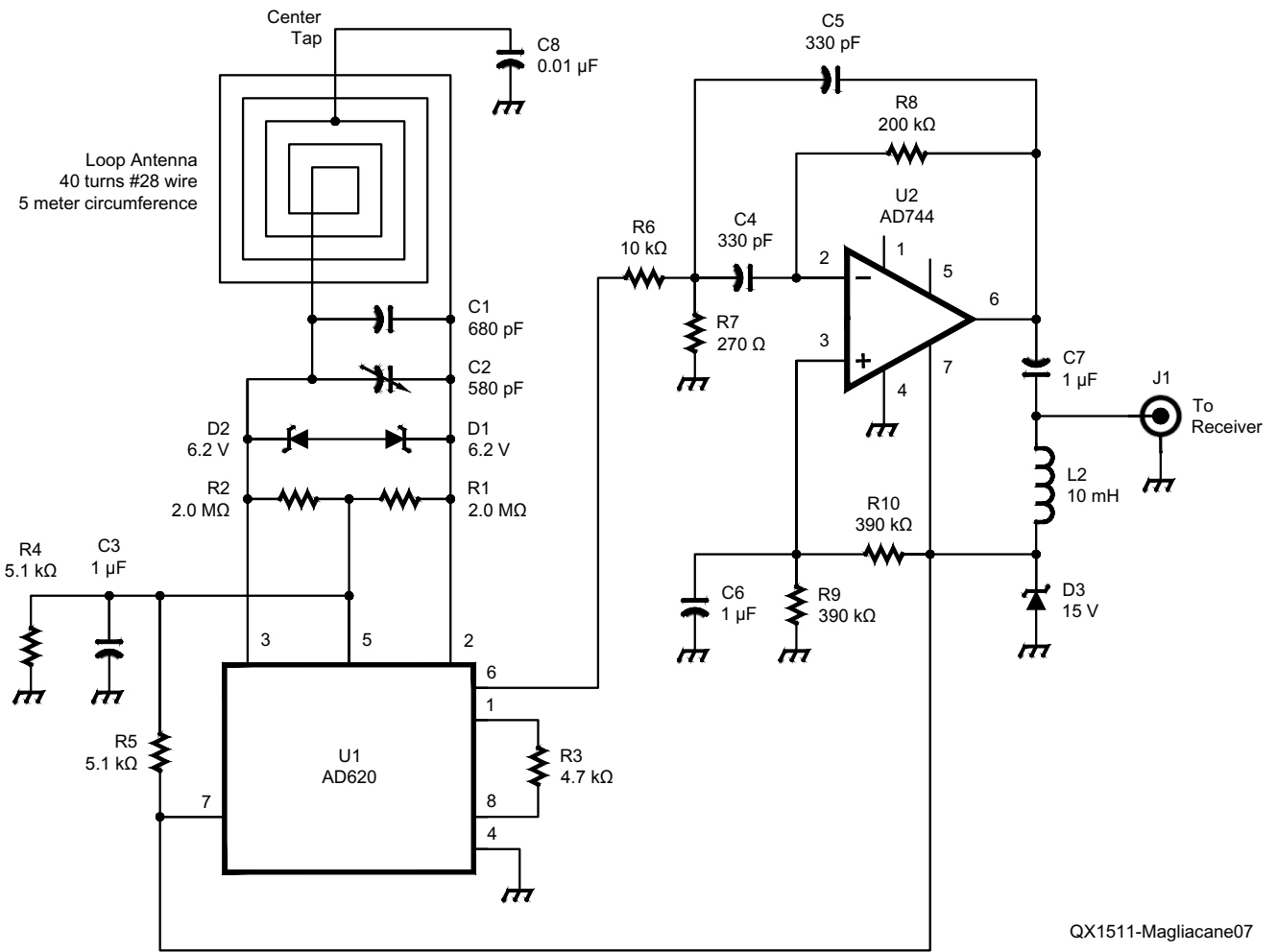


Figure 7 — 60 kHz WWVB loop antenna preamplifier. In addition to providing 40 dB of gain, the preamp properly interfaces the balanced loop antenna with the ground-referenced circuitry in the frequency standard.

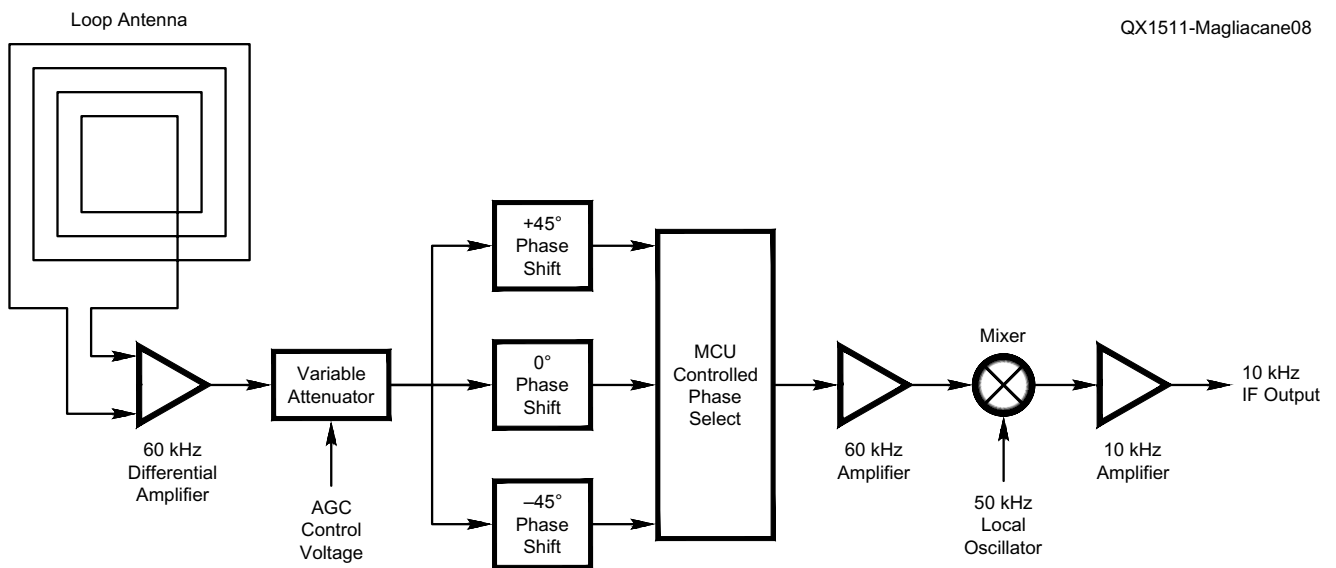


Figure 8 — This block diagram illustrates the overall RF to IF conversion process. The +45° and -45° phase shift networks were used in the past to compensate for the WWVB hourly phase signature, but have not been required since the introduction of BPSK modulation was made in 2012.

power from the frequency standard through the same length of coax. This connection provides a voltage transfer rather than a power transfer of RF energy between the preamplifier and the frequency standard. Since the length of coax will be small in terms of wavelength, transmission line effects and impedance matching concerns can be ignored, and coaxial cable of any convenient surge impedance can be employed.

The amount of capacitance required in parallel with the loop to achieve resonance at 60 kHz depends on the size, shape, distributed capacitance, and overall inductance of the loop. The 40 turn loop described here required about 1050 pF of capacitance. Capacitor C1 should be a silver mica or similar low-loss, temperature stable capacitor. I used an Elmenco 467 110 pF to 580 pF compression trimmer capacitor at C2 to carefully bring the loop to resonance at 60 kHz.

Signal-to-noise ratios at LF are often enhanced by desensitizing the near-field response of the receiving antenna to E-Field energy. This effect is often accomplished by employing an electrostatic shield around the perimeter of the loop. In this design, E-Field desensitization is achieved by employing a high common-mode-rejection differential amplifier as the first stage of the preamplifier. Capacitor C8 provides an AC ground to the electrical center of the loop, to enhance the preamplifier rejection of out-of-band signals. Zener diodes D1 and D2 help protect the Analog Devices AD620 differential amplifier from damage when nearby lightning strikes induce high voltage impulses across the antenna.

The differential amplifier is followed by a 60 kHz second-order active bandpass filter designed around an AD744 operational amplifier. This stage provides additional RF selectivity beyond that of the loop antenna alone, and raises the overall voltage gain of the preamplifier to 40 dB. The AD744 has the capability of driving capacitive loads, and can deliver output voltages as high as $10 V_{pp}$ without distortion.

Resistor R3 sets the gain of the AD620, and may be increased in value if less preamplifier gain is desired. For best performance, capacitors C4 and C5 should be low-loss, high temperature stability devices (such as silver mica), and all resistors should be within 5% tolerance.

RF Amplitude and Phase Management

Figure 8 illustrates the overall process of converting the WWVB 60 kHz signal down to a 10 kHz IF, where separate amplitude and phase detection takes place. Figure 9 illustrates the frequency standard RF circuitry in greater detail.

Inductor L1 and capacitor C1 form a bias tee network that feeds DC operating voltage to the preamplifier while simultaneously directing RF from the preamplifier into a current controlled RF attenuation network. This network is part of the frequency standard AGC circuitry, and it consists of resistors R1 and R2, and diodes D1 through D4.

Capacitor C6 along with diodes D5 and D6 and resistor R13 charge capacitor C7 to the peak level of the IF voltage. Analog switch U2A is opened when strong atmospheric discharges are detected. This action prevents C7 from charging to the peak level of the noise impulse, which would otherwise engage the AGC more heavily, and desensitize the frequency standard in the moments following the static crash.

The voltage across C7 is buffered by op-amp U3C, level shifted through diodes D7 and D8, and used to control the RF attenuation network through transistors Q1 and Q2.

With no current applied to the network, the dynamic resistance of all four diodes is high, and very little RF signal attenuation takes place across resistors R1 and R2. As the IF signal level begins to rise above the threshold set by diodes D7, D8, and the base-emitter junctions of transistors Q1 and Q2, the DC current passing through diodes D1 through D4 begins to increase. This current decreases the dynamic resistance of the diodes, and causes an increasing amount of RF to be conducted through them to ground. A fairly constant peak RF level remains after the attenuation network, and appears on the emitter of transistor Q3.

For many decades, WWVB employed a method of station identification where its transmitter would advance the phase of its carrier $+45^\circ$ 10 minutes after the start of each hour, and return to normal phase 5 minutes later. These hourly phase shifts were discontinued when BPSK modulation was added in 2012. Nevertheless, the circuitry used to compensate for these phase shifts worked extremely well, and is included here for discussion.

60 kHz RF appearing on the emitter of transistor Q3 is simultaneously applied to a $+45^\circ$ phase shift network (C3, R10), a -45° phase shift network (R8, C4), and a resistive voltage divider (R6, R7) having the same attenuation characteristic as each phase shift network. In the past, the appropriate RF path would be selected by the microcontroller based on the current time of day. The 0° path would normally be selected when the frequency standard was initially powered on. At 10 minutes after the hour, the -45° path would be selected through analog switch U10C and into U10B to compensate for the $+45^\circ$ phase advance that would occur at that time. At 15 minutes after the hour, the 0°

path would again be selected through U10B. If the frequency standard were powered on between 10 and 15 minutes past the hour, the WWVB carrier would have already been advanced $+45^\circ$. Therefore, the frequency standard would continue using the 0° path, and later select the $+45^\circ$ path when WWVB would have shifted back -45° at 15 minutes after the hour.

Converting to a 10 kHz IF

Phase and amplitude conditioned 60 kHz signals are next handled by the circuitry illustrated in Figure 10. Here, additional RF gain and selectivity are provided by active bandpass filters designed around op-amps U1A and U1B. As was the case in the preamplifier, the 330 pF capacitors at C11, C12, C14, and C15 should be of a temperature stable, low-loss chemistry. An AGC conditioned 60 kHz RF sample from the output of U1A is buffered and made available for use outside the frequency standard.

U4C forms a 180° unity gain phase inverter that forms a balanced mixer along with U5A, one section of a CD4053BE triple SPDT analog switch. Driven by a 10 MHz derived 50 kHz local oscillator, this mixer converts the 60 kHz RF signal down to a 10 kHz IF. Op-amps U4A, U4B, and U4D form a 10 kHz biquad active bandpass filter that serves as a high-gain, narrow bandwidth IF amplifier. This amplifier provides 46 dB of gain and a 3 dB bandwidth of 100 Hz. The center frequency of the amplifier is set to 10 kHz through careful alignment of potentiometers R36 and R39. The 330 pF capacitors employed at C18 and C19 must be of a low-loss variety.

Working from within the AGC loop, the IF amplifier provides an output voltage of about $8 V_{pp}$. A sample of the 10 kHz IF is made available for use outside the frequency standard.

Demodulating “I” and “Q”

The 10 kHz IF signal is split between a straight-through path and a path through op-amp U6B that produces a -90° phase shift. A balanced mixer — consisting of op-amp U6C and analog switch U5B — is driven by a 10 MHz derived 10 kHz local oscillator, and forms an in-phase (“I” channel) demodulator. The -90° phase shifted path feeds a second balanced mixer consisting of op-amp U6C and analog switch U5C. This mixer is driven by the same 10 kHz local oscillator after it has passed through exclusive OR gate U27A, and produces a quadrature (“Q” channel) demodulator.

The output of the “I” channel demodulator is a $+6 V$ referenced baseband DC voltage that is linearly proportional to the WWVB

carrier phase polarity and modulation amplitude. After the effects of BPSK modulation have been removed by the action of U27A and its associated circuitry, the “Q” channel demodulator produces a +6 V referenced baseband DC voltage that is linearly proportional to a WWVB carrier having no phase modulation.

Figure 11 presents an overview of the signal path taken by the 10 kHz IF. As illustrated in Figure 12, op-amps U3D and U7D function as a 3.685 Hz wide four pole Bessel low-pass filter, and set the frequency standard “I” channel RF bandwidth to 7.37 Hz. Output from the filter drives op-amps U25A and U25B. Using a virtual ground DC reference of +6 V, op-amp U25A acts as a voltage comparator and demodulates the WWVB BPSK into a 12 V_{p-p} square wave. U25B serves as a unity gain phase inverter, and provides an “I” channel waveform that is complementary to the original.

The CD4066B analog switching arrangement that follows is driven by the demodulated BPSK waveform provided by U25A. By selecting the non-inverted “I” channel signal through U26B when the WWVB carrier phase is normal, and selecting the inverted “I” channel signal through U25B and U26C when the WWVB carrier phase is inverted, a BPSK-free “I” channel is produced. U25A’s BPSK correction signal is also applied to exclusive OR gate U27A to control the phase of the 10 kHz local oscillator fed to the “Q” channel demodulator, and allows the demodulator to maintain a constant output polarity.

The filtered and BPSK-free “I” channel energy is applied to op-amp U7A and diode D9, and work through analog switch U10A and resistor R57 to charge capacitor C27 to the peak voltage of the demodulated AM time code. This voltage is buffered through U7B, whose output is applied across the R59/R60 voltage divider. The voltage divider sets the threshold of comparator (op-amp) U7C to a level that is midway between the upper (0 dB peak reference) and lower (-17 dB below peak reference) amplitudes of the WWVB detected carrier. The comparator produces a switching waveform that illuminates green Time Code LED, D10, in synchronization with the WWVB amplitude modulation. This waveform is also made available to the microcontroller following a translation to TTL voltage levels by transistor Q6.

Analog switch U10A is briefly opened when high amplitude noise impulses are detected to prevent them from charging C27 and overshooting the decision threshold set by U7C. The demodulated time code pulses and the peak time code voltages are also indicated on a meter mounted on the front panel of the frequency standard’s enclosure.

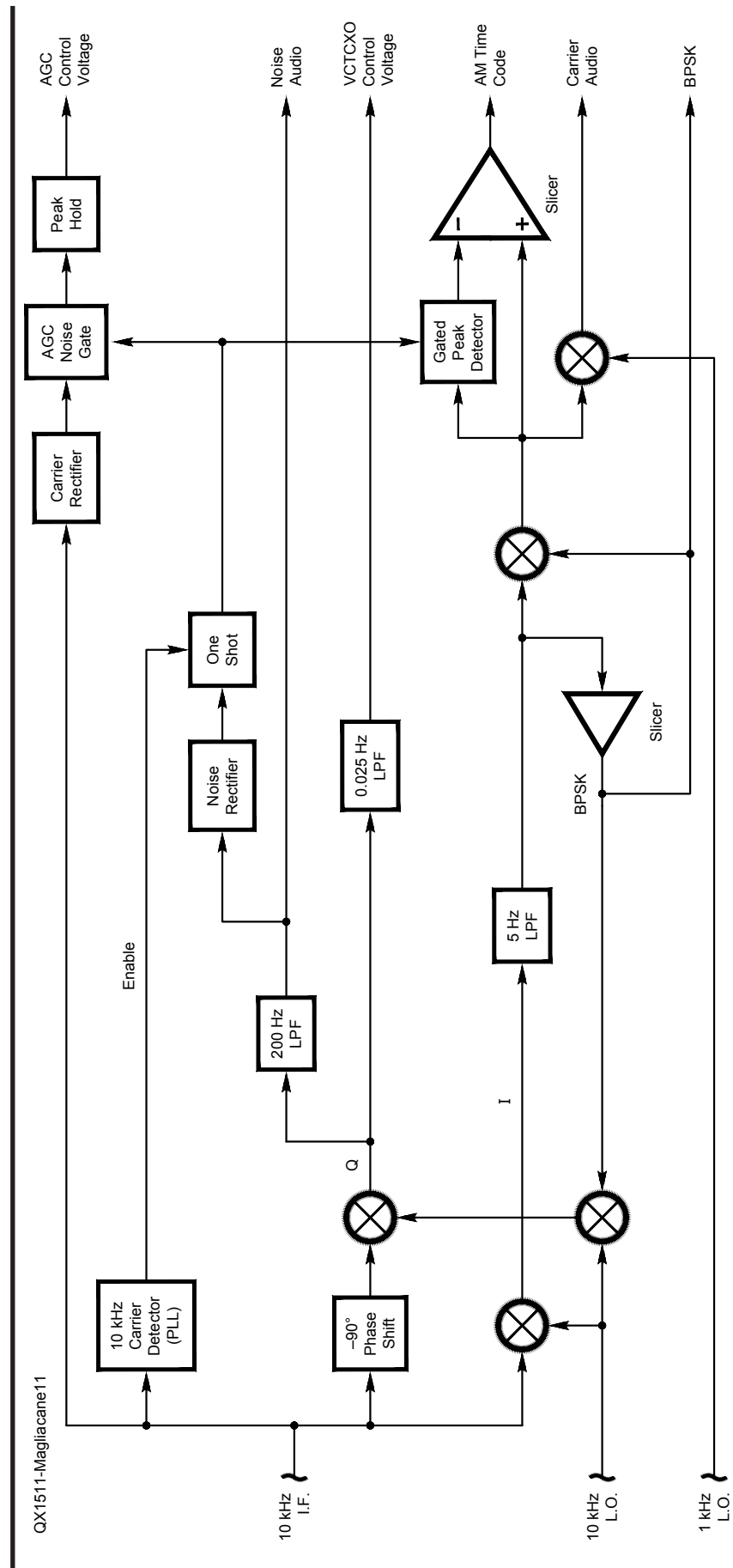
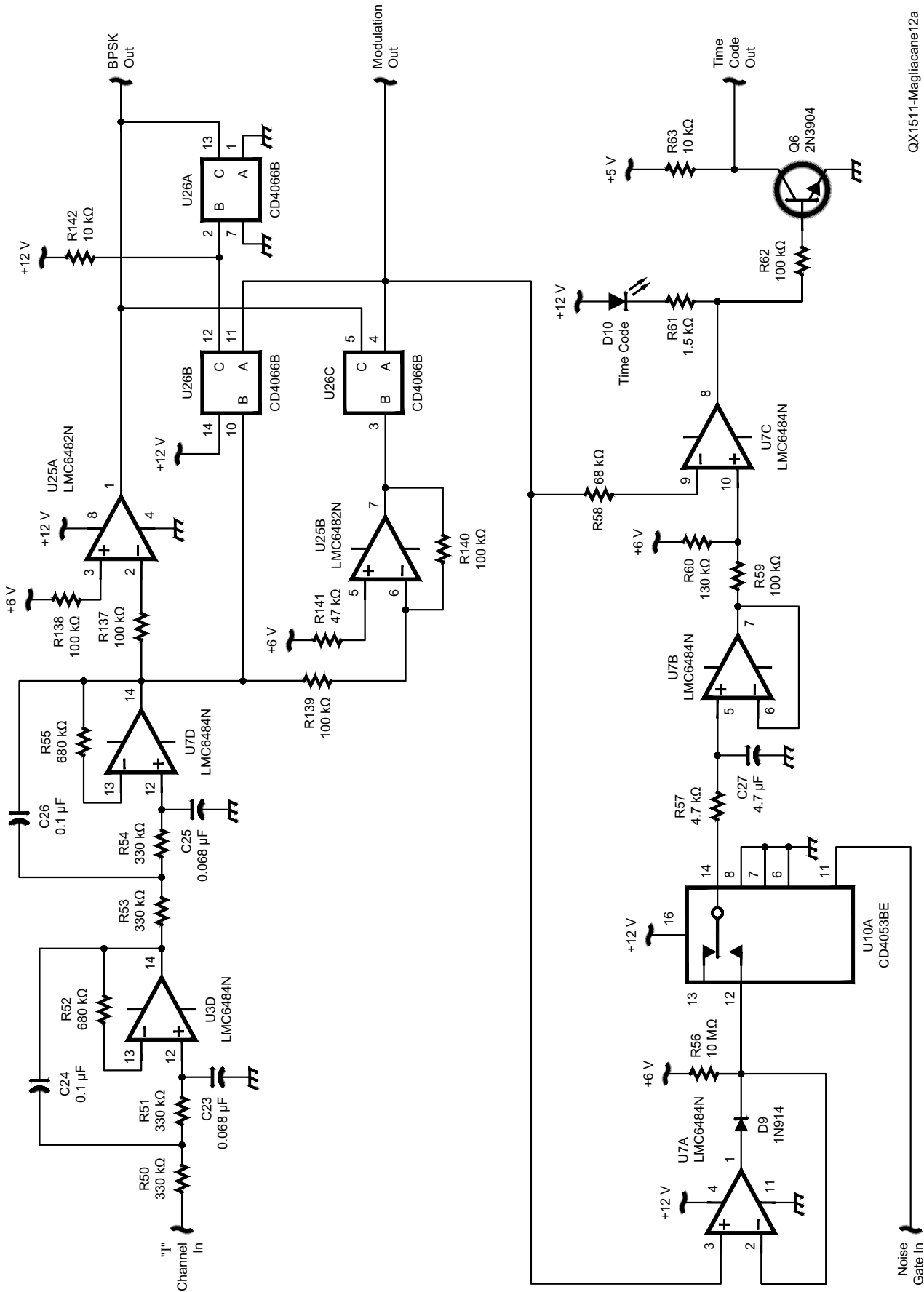
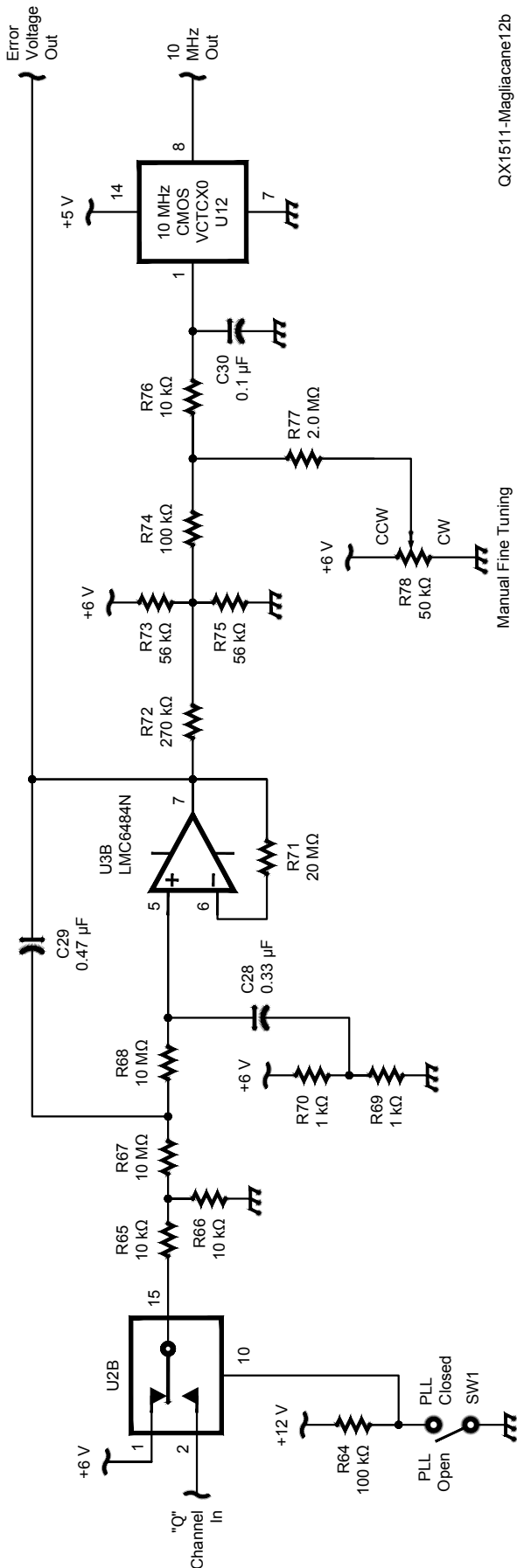


Figure 11 — This block diagram illustrates the post-detection processing. The WWVB amplitude shift keying and phase shift keying are demodulated from the I channel while the Q channel provides tuning voltage for the VCTCXO.



QX1511-Magliacane12a



QX1511-Magliacane12b

Manual Fine Tuning

Figure 12 — This schematic diagram shows the details of the I and Q channel filtering and processing. Both amplitude and phase shift keying signals are demodulated from the I channel, while the Q channel develops the tuning voltage that forces the 10 MHz oscillator to track the phase of the WWVB carrier.

Controlling The VCTCXO

After passing through analog switch U2B, the output of the “Q” channel demodulator is fed through a 0.025 Hz wide second order low-pass filter (U3B) before being applied to the 10 MHz VCTCXO. Low leakage, metalized polypropylene film capacitors were employed at C28 and C29.

The resistive network between the low-pass filter and the VCTCXO exhibits 21 dB of attenuation, and controls the VCTCXO tuning sensitivity and the maximum loop gain of the frequency standard. The loop gain setting is fairly critical, since a third-order phase-locked loop (PLL) function is produced by the VCTCXO and the second order low-pass filter that precedes it. Third-order PLLs offer superior noise rejection and lower steady-state errors than second order PLLs, but they do so with a reduced phase margin. Since the VCTCXO will be generally close to its target frequency, acceptable overall loop stability is achieved by simply keeping the PLL loop gain no higher than that necessary to electronically steer the VCTCXO to exactly 10 MHz over a limited tuning range. If greater amounts of steering voltage are required, a front panel mounted 10 turn potentiometer (R78) is available to allow manual fine tuning of the oscillator. Switch SW1 allows manual tuning to take place either with (PLL Closed) or without (PLL Open) there being a tuning influence from WWVB. Changing SW1 to a DPDT switch and adding a red LED and an appropriate current limiting resistor can be advantageous in providing a visual cue to the user that the PLL switch is in the open position.

This frequency standard employs a Bomar Crystal Company model B17025-ADMF-10.000 10 MHz VCTCXO as its master oscillator. The oscillator operates on 5 V, and has a frequency stability of 2.5 ppm. It provides an HCMOS square wave output waveform, and has a measured positive slope tuning sensitivity of 62.8 Hz/V. In addition to being voltage controlled, the oscillator also possesses a trimmer capacitor to permit coarse frequency adjustments to be made independent of the tuning voltage applied to the oscillator. Since this frequency standard operates the oscillator with a nominal tuning voltage close to 3.0 V rather than the 2.5 V ($+V_{cc}/2$) typically expected in a 5 V oscillator, the trimmer allows oscillator adjustment to 10 MHz with this higher tuning voltage applied.

Since the PLL loop gain in this frequency standard is intentionally low, and some dependence on manual tuning is sometimes required, a more stable oscillator would make manual tuning adjustments far less critical when changes in ambient temperature take place.

LO and Standard Frequency Generation

Figure 13 illustrates the circuitry used to buffer the 10 MHz VCTCXO for external applications, and divide it down in frequency for both internal and external use. U18, a Microchip MCP101-460HI/TO active high supervisory circuit, holds the active high CLEAR inputs of every 74HC390 dual decade counter high for approximately 350 ms after the frequency standard is first powered on. In addition, U15A and U15B at the far end of the divider chain are reset independently of the other dividers by the microcontroller in alignment with the

beginning of the UTC second, shortly after the frequency standard is first powered on.

Buffered TTL level outputs at 10 MHz, 1 MHz, 100 kHz, 50 kHz, 25 kHz, 10 kHz, 1 kHz, and 100 Hz are available through U17, a 74HC151 multiplexer. Frequency selection takes place through a three bit binary code applied to the multiplexer data select lines. An eight position BCD switch, or simply a three pole eight position rotary switch wired with the appropriate ground connections and pull-up resistors can be used to select the output frequency. Two additional buffered 10 MHz outputs are also provided.

Figure 14 illustrates the circuitry associated with the microcontroller, back-lit LCD alphanumeric display, RS-232 port, and several regulated voltage references and sources used by the frequency standard. The PIC16F88 (U11) accepts the WWVB AM time code, the WWVB BPSK time code, a 10 Hz timing signal from the frequency dividers, filtered PLL error voltage derived from the "Q" demodulator, and a DC reference voltage that is exactly half the +6 V used throughout the frequency standard as a virtual ground.³ The microcontroller generates the reset pulse that clears 74HC390 decade counters U15A and U15B as previously described. It also generates the signals necessary for driving the legacy $\pm 45^\circ$ RF phase shift networks in the front end of the frequency standard, the 24×2 LCD, and provides serial UTC date and time information to peripheral devices through a Dallas DS232A RS-232 level converter (U9).

Figure 15 illustrates the audio, loss of signal, noise detection, and noise mitigation circuitry. A DC voltage from the "I" channel demodulator that is proportional to the WWVB modulation amplitude is applied to analog switch U2C, where it is modulated at a 1 kHz rate to produce an amplitude modulated audio tone. A narrow bandpass filter following the modulator attenuates the level of harmonics contained in the 1 kHz switching carrier. The resulting sinusoidal waveform is applied to an audio select switch before being made available to an LM380 audio power amplifier.

Noise Detection and Mitigation Circuitry

While the "I" channel contains a DC voltage proportional to the WWVB modulation amplitude, the output of the "Q" channel (after BPSK-correction) is modulation free. Therefore, any rapid modulation of the DC voltage present on the output of the "Q" demodulator is the result of noise energy present at 60 kHz. The circuitry surrounding transistor Q7 forms a 200 Hz wide low-pass filter that rejects any high frequency energy remaining from the "Q" channel demodula-

tion process that might take on the appearance of noise to the circuitry that follows.

The low-pass filter feeds a precision full-wave rectifier designed around op-amps U20A and U20B. The rectifier feeds negative-going noise impulses to U22, an LM555 monostable multivibrator. The triggering threshold for the LM555 is set through potentiometer R97, and is adjusted so that the LM555 triggers only when strong lightning discharges are detected. Once triggered, the LM555 lights D13, an amber colored LED, to indicate noise detection. The 555 also opens the analog switches associated with the AGC (U2A) and peak time code detection (U10A) circuitry to prevent their reaction to the static crash. The rectified noise voltage also drives a front panel meter to provide indications of its relative intensity.

The 200 Hz low-pass filter also provides an audio signal to the LM380 audio amplifier to permit aural monitoring of any 60 kHz background noise that could influence reception quality. U19, an LMC567 tone decoder PLL, monitors the 10 kHz IF and responds to the absence of the WWVB carrier. The LMC567 lights D14, a red colored LED, if a loss of signal condition is detected. It also holds the LM555 in reset mode, and prevents it from lighting the noise LED and opening the noise-gated analog switches under a loss of signal condition, or during the first few seconds after power-up while the AGC becomes fully acclimated to the WWVB signal level.

Multimeter and Sinusoidal Outputs

Figure 16 illustrates the circuitry responsible for providing sinusoidal output signals and analog meter indications. A fourth order 1 kHz bandpass filter designed around op-amps U20C and U20D filter the 1 kHz square wave local oscillator signal into a sinusoidal waveform. This waveform is amplified by U23, an LM386 audio power amplifier that provides sufficient output current to drive a low impedance load.

Op-amp U6D buffers a sample of the 10 kHz IF, U1D buffers a sample of the 60 kHz RF signal, and together these signals are made available for external use. The gain of each buffer has been tailored to produce RF and IF output samples of relatively equal amplitudes.

SW3, a two pole four position rotary switch allows relative measurements of modulation level, peak signal level, center tuning, and ambient radio noise levels to be made through a single 100 μ A D'Arsonval panel meter.

The Liquid Crystal Display

The PIC16F88 contains a 10 bit analog-

to-digital converter that is used to measure the relative WWVB-derived error voltage fed to the VCTCXO. This voltage is represented as a three digit number between -512 and +511, and is continuously displayed on the bottom center of the LCD. Proper adjustment of the VCTCXO through R78 is achieved when a stable reading close to 000 is made.

The PIC A/D converter has a resolution of 6 V/1024 or 5.86 mV. Since the error voltage is attenuated by a factor of 11.3 (21 dB) before it reaches the VCTCXO, but is read by the PIC prior to this attenuation, the tuning indicator is able to resolve a 518 μ V change in the VCTCXO error voltage.

Power Up Procedure

Once powered on, the frequency standard sequences through several modes of operation before it is finally ready for use. The setup process takes several minutes to complete, and the LCD keeps the user informed of the process along the way.

The display illustrated in Figure 17A appears when the frequency standard is first powered on. The microcontroller firmware version is briefly displayed on the first line, while the VCTCXO digital tuning indicator permanently appears in the middle of the line below.

After several minutes have passed and the frequency standard VCTCXO has become locked in phase with that of the WWVB carrier, the microcontroller begins timing the interval between each WWVB amplitude carrier reduction. Carrier reductions occur at the start of each UTC second, and once eight successive properly timed carrier reductions have been detected, the display switches to that illustrated in Figure 17B. When this change occurs, the microcontroller begins looking for the Marker bit sequence, identifying the conclusion of the current time code frame and the beginning of the next.

While waiting for the next frame to begin, the display indicates the phase of the WWVB carrier (+ or -) and the identity of each time code bit (0, 1, or M) received over the previous second. If the bit cannot be identified, a "?" character is displayed.

Since the WWVB carrier level is always "low" for the first 200 ms of every second, and always "high" for the last 200 ms of every second, these intervals carry no time code information and are ignored by the microcontroller bit correlation decoding algorithm. These predictable amplitude levels are instead used to estimate the quality of time code reception, which is displayed as a single digit between 0 (poor) and 8 (excellent) to the right of the time code bit.

Once the beginning of the frame is found, the display switches to that shown in Figure 17C. The microcontroller starts a process

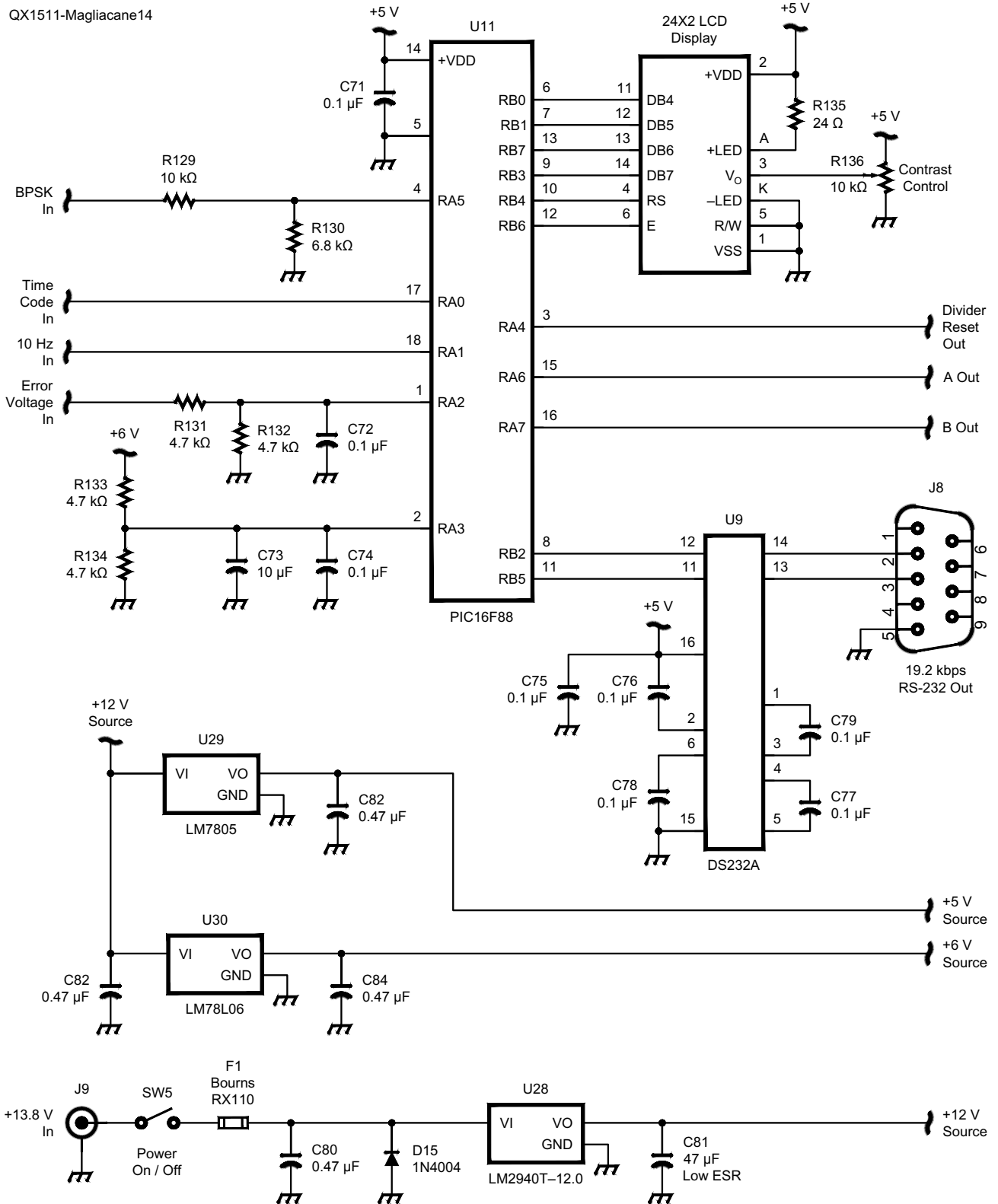
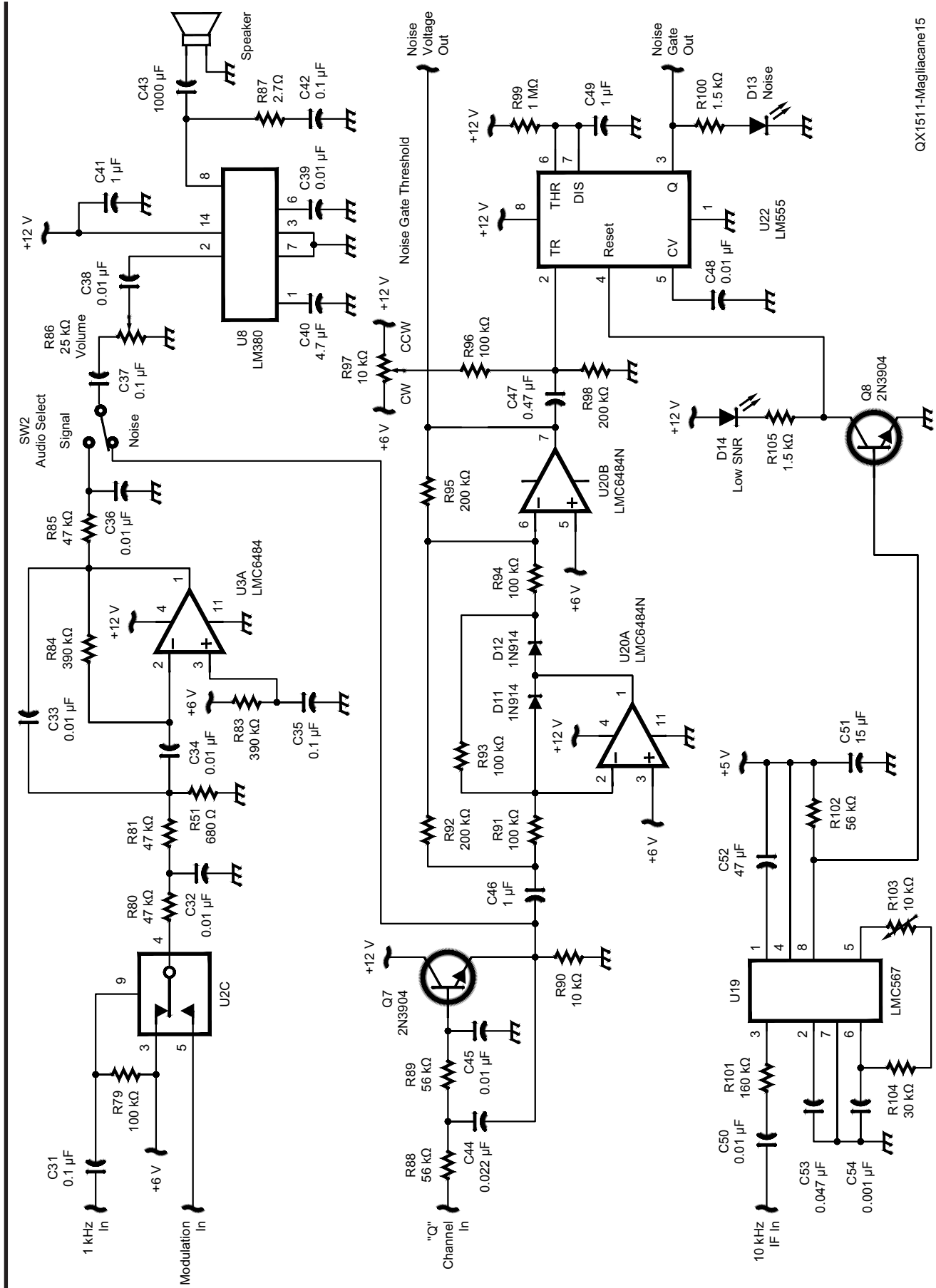


Figure 14 — A PIC microcontroller decodes the WWVB time code, functions as a real-time UTC clock driven by the disciplined oscillator, and provides date and time of day information via the liquid crystal display and RS-232 serial port.



QX1511-Magliacane15

Figure 15 — Here is the schematic diagram for the audio and noise signal processing. Baseband WWVB signals modulate a 1 kHz carrier for aural monitoring of the signal. Noise impulses detected on the Q channel trigger a noise gate that temporarily inhibits AGC action and time code detection. Noise energy can also be monitored through the audio amplifier.

in which it begins decoding the frame and evaluating the integrity of the data being collected. A countdown timer representing the number of seconds until the completion of this process is displayed on the top right hand side of the display. If the data collected looks reasonable, a real-time clock/calendar operating within the firmware of the microcontroller is set to the time and date decoded.

The microcontroller then looks for validation of the information received by examining the next frame of data, and compares the result with that of the real-time clock one minute later (Figure 17D). If the received time and date match that of the clock, then the microcontroller begins displaying the locally running clock and calendar from that point forward. See Figure 17E. If the validation fails, then the process reverts to the point illustrated in Figure 17C, in which the reception and validation routines are repeated until the current time and date are finally confirmed.

Once the validation process is complete, the frequency standard begins sending the current UTC time and date, once every second, to any connected peripherals via the RS-232 port (Figure 18). These peripherals might include a PC with a real-time clock that can be set through appropriate software, or an external digital clock display. While this frequency standard is not intended to serve as an NIST-traceable time source, the date and time reported through both the serial port and the LCD are advanced by 100 ms to compensate for the nearly equal amount of signal processing delay inherent within the electronics in the frequency standard.

Parts and Construction

This frequency standard was developed and tested in discrete stages over a period of several years. Due to this modular design

approach, much of the circuitry was built on a series of 95 × 70 mm and 70 × 45 mm perforated circuit boards that have all been interconnected to one another to form a complete unit. Figure 19 is a view inside the cabinet of my unit. With the exception of the DC power supply, antenna, and remote RF preamplifier, all circuitry is housed in a single Ten-Tec model BK-1249 enclosure that measures 12 inches × 4 inches × 9 inches (HWD) Figure 20 is a photo of the front of the unit.

In an effort to enhance frequency stability, thermal effects caused by heat dissipation of the frequency standard electronics are minimized by keeping the DC power supply physically removed from the enclosure, and by mounting both the LM2940T-12.0 and the LM7805 voltage regulators to the enclosure's back panel. The greatest single sources of heat outside of the voltage regulators are the LCD backlight, and interestingly enough, the VCTCXO, itself.

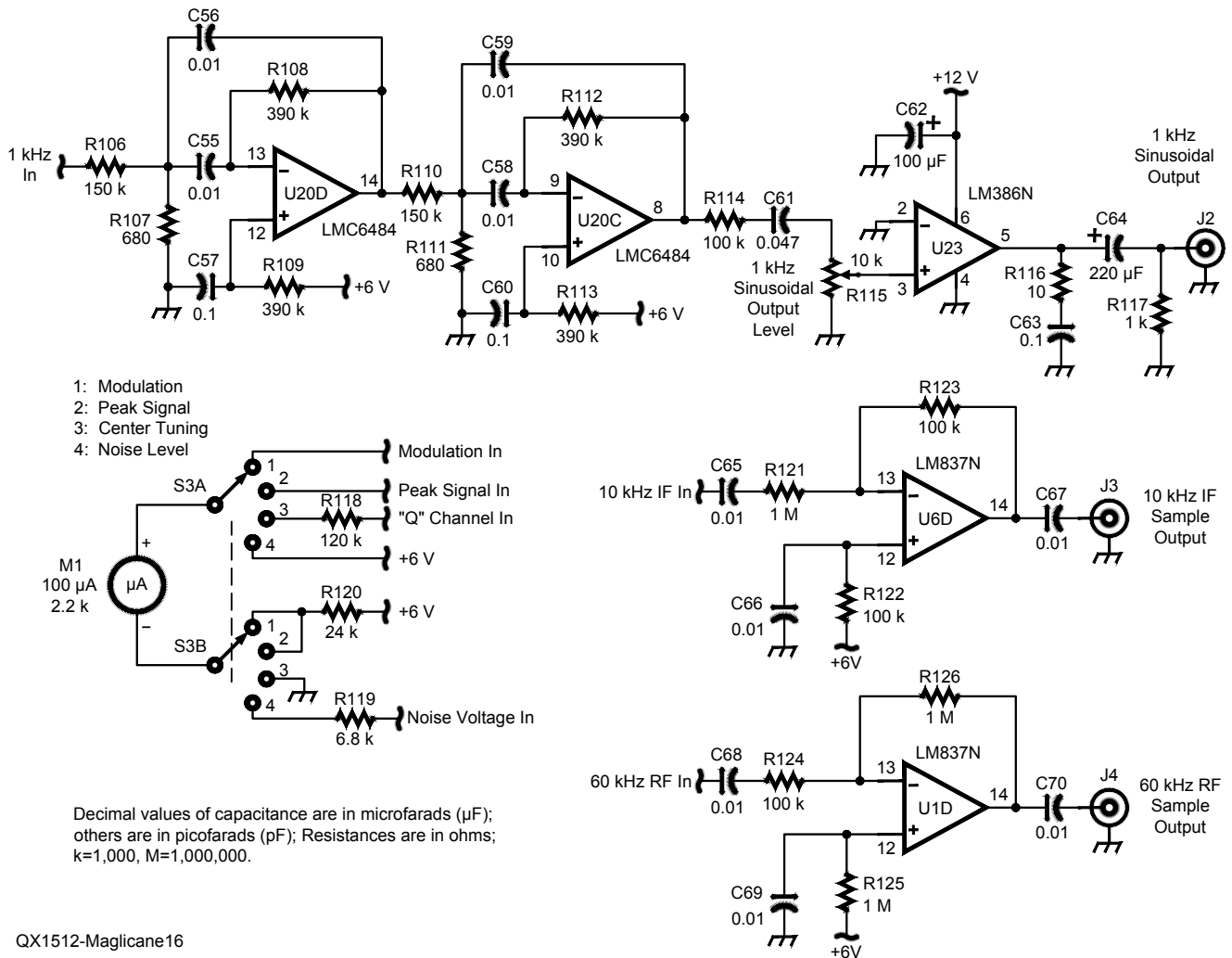


Figure 16 — Metering and various sinusoidal output signals are shown on this schematic diagram. In addition to providing buffered 60 kHz RF and 10 kHz IF samples, a precise 1 kHz sinusoidal waveform capable of driving a small speaker is provided.

Alignment and Testing

The frequency standard may be powered from any 13.8 V DC power source capable of supplying at least 300 mA of current. A Bourns RX110 resettable fuse (F1) located after the power switch is followed by a reverse biased silicon diode to ground (D15). These are used as safety measures to help to protect the circuitry from damage should an over-current or reverse polarity condition ever occur.

The antenna can be adjusted to achieve resonance at 60 kHz by monitoring the output of U1 (AD620 Pin 6) with an oscilloscope while radiating a weak signal at 60 kHz from a nearby function generator and varying the amount of capacitance in parallel with the loop to achieve maximum response. Table 1 provides equations for determining the voltage produced by the loop given its physical dimensions, electrical properties, and local field strength.

Receiver alignment should begin by first adjusting the Manual Fine Tuning Control (R78) until the DC voltage between its wiper and ground reads exactly half that of the +6 V reference.

Next, with the antenna and preamplifier disconnected from the frequency standard, switch SW1 to the “PLL Open” position, and adjust the coarse frequency adjustment capacitor on the VCTCXO until it operates as close to 10 MHz as possible. Being able to obtain a close zero-beat with WWV should be more than adequate at this stage of the alignment.

With the Audio Source Switch (SW2) in the “Noise” position and the 60 kHz function generator off, connect the antenna and preamplifier to the frequency standard. Carefully adjust potentiometers R36 and R39 simultaneously for maximum noise level.

Operation

With the plane of the loop antenna oriented in the direction of Fort Collins, Colorado, final alignment of the VCTCXO can take place. Manual coarse tuning can be achieved by placing SW1 in the “PLL Open” position, and Meter Function Switch (SW3) in the “Center Tuning” position, while slowly adjusting the Manual Fine Tuning control (R78) for a steady, center reading on meter M1.

Table 1

Equations that relate the voltage produced by an electrically small (<0.08 λ) air-core loop antenna to the local field strength given the loop’s physical dimensions and electrical properties.

$$E_s = \frac{2\pi eNA}{\lambda}$$

$$e = \frac{E_s \lambda}{2\pi NA}$$

$$Q = \frac{f_r}{bw}$$

$$E_o = QE_s$$

Where:

E_s = voltage induced into the loop (μV).

E_o = loop output voltage at resonance (μV).

f_r = loop resonant frequency (Hz).

bw = 3 dB bandwidth (Hz)

Q = the Q of the loop.

e = local field strength (μV/m).

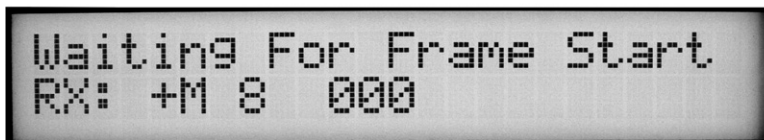
N = number of turns.

A = enclosed area of the loop (square meters).

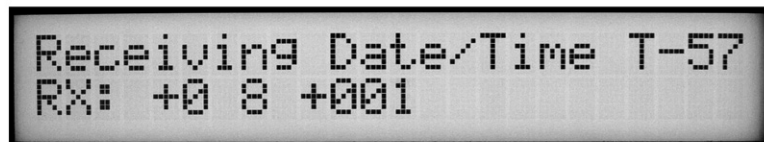
λ = wavelength (meters).



(a)



(b)



(c)



(d)



(e)

Figure 17 — These images show the various LCD screens depicting each of the five stages of frequency standard operation following power up. The final stage is where the UTC date and time are continuously displayed and made available to peripheral equipment via the RS-232 port.

23:59:48 08/04/14
 23:59:49 08/04/14
 23:59:50 08/04/14
 23:59:51 08/04/14
 23:59:52 08/04/14
 23:59:53 08/04/14
 23:59:54 08/04/14
 23:59:55 08/04/14
 23:59:56 08/04/14
 23:59:57 08/04/14
 23:59:58 08/04/14
 23:59:59 08/04/14
 00:00:00 08/05/14
 00:00:01 08/05/14
 00:00:02 08/05/14
 00:00:03 08/05/14
 00:00:04 08/05/14
 00:00:05 08/05/14
 00:00:06 08/05/14
 00:00:07 08/05/14

Figure 18 — At the beginning of every second, the 19.2 kbps RS-232 serial port provides the current UTC time and date in the form of HH:MM:SS MM/DD/YY followed by a line feed and carriage return.

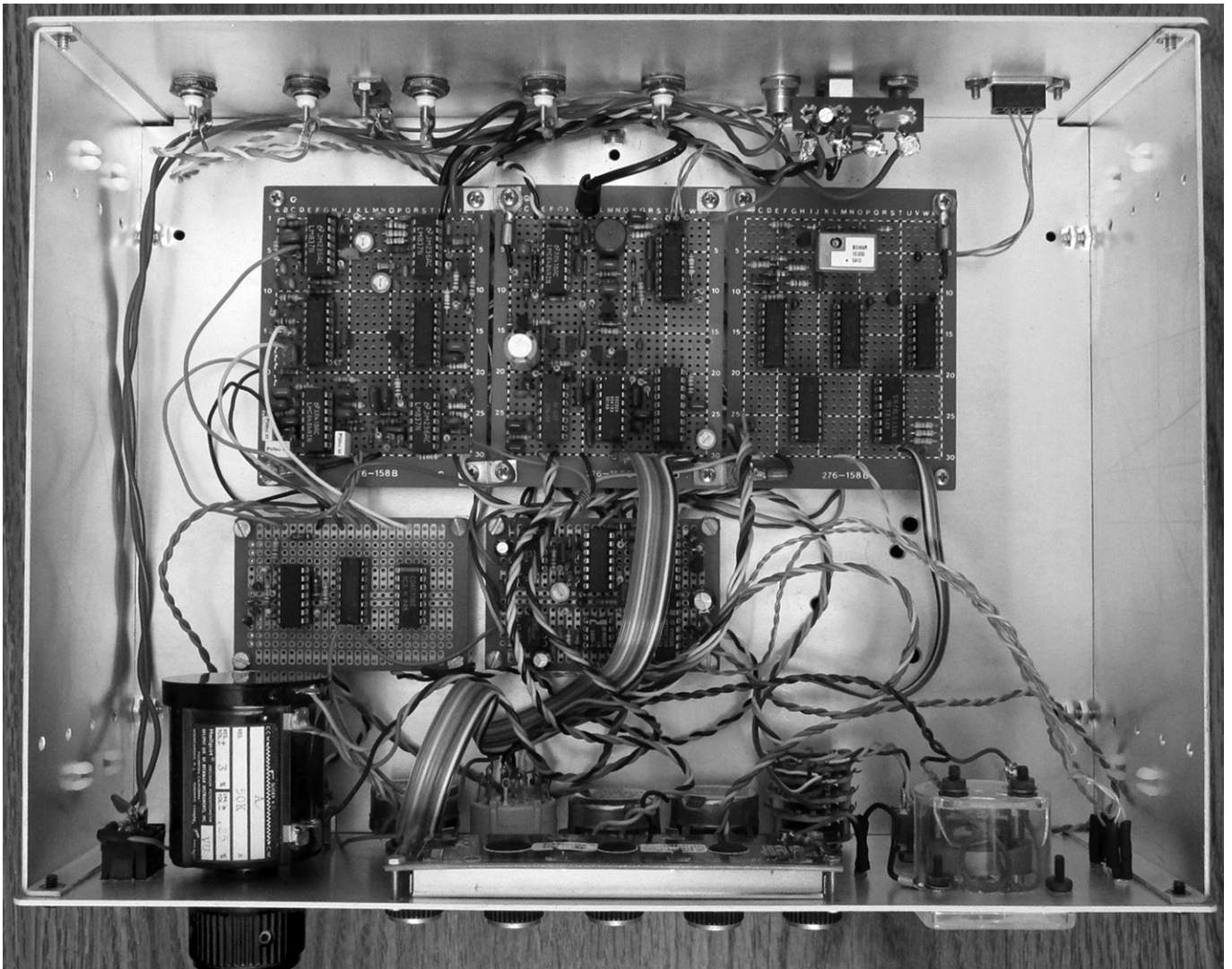


Figure 19 — The frequency standard was designed using a modular approach that employed separate perforated circuit boards for various device functions. This approach provided a convenient way to add circuitry as the design evolved over time.



Figure 20 — Front view of the frequency standard in operation. The large knob on the upper left permits manual fine tuning of the VCTCXO, while the display provides the UTC date and time.

Placing the audio source switch (SW2) in the “Signal” position will help verify that WWVB reception is taking place. If all has gone well, placing SW1 in the “PLL Closed” position should allow the VCTCXO to slowly move into phase alignment with the WWVB carrier. Minor adjustments of the VCTCXO can be made at this point to bring the LCD tuning indicator reading to as close to 000 as possible.

After several minutes of reception have transpired, the LCD sequence illustrated in Figure 17 will begin to take place. If high local noise levels impair reception of the WWVB time code, the antenna may need to be reoriented to place the noise source in one of the two antenna pattern nulls. Placing the Meter Function Switch in the “Noise Level” position will permit the relative ambient noise level to be displayed on the meter. Placing the Audio Source Switch in the “Noise” position will allow the noise level to be monitored through aural means without having to keep an eye on the meter for visual cues.

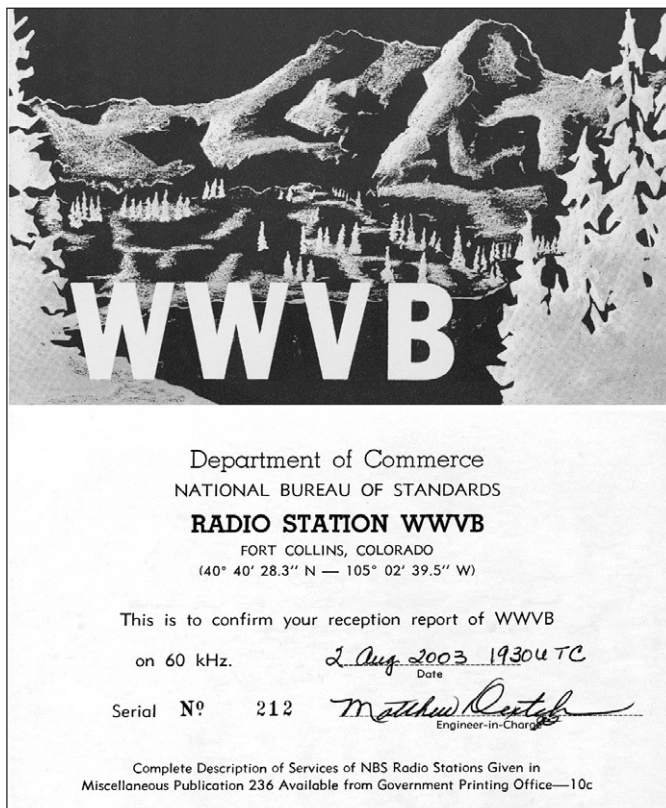


Figure 21 — The ability to receive and successfully identify distant radio signals remains a source of pride for many radio enthusiasts. While formal confirmation of GPS satellite reception may not be possible, radio station WWVB offers QSL cards to validate reception reports.

Summary

While some may question the merit of employing WWVB as a frequency reference at a time when GPS-disciplined frequency standards are so ubiquitous, similar questions could be raised about the relevance of the Amateur Radio Service in a world dominated by cellphones and the Internet. The frequency standard described here employs a “purely RF” approach toward disciplining a local oscillator against an extremely accurate national atomic standard. It was developed not only to create a laboratory grade frequency standard, but to do so while pursuing a life-long interest and fascination with the underlying radio concepts that make such a process possible. Figure 21 shows a reception QSL that I received from WWVB in 2003.

While not a state-of-the-art device by twenty first century standards, the frequency reference described here will likely provide more than adequate performance for many modern engineering, research, and scientific purposes. For those possessing GPS-disciplined standards, this frequency

standard can provide a reliable sanity check as well as a redundant backup.

The recent changes made to the WWVB broadcasts by the National Institute of Standards and Technology have been unsettling for some individuals. What these actions reveal, however, is that while the WWVB primary role is changing, it is changing because its use is growing, and this growth will help ensure there is strong support for keeping WWVB on the air for decades to come. See you in the next FMT!

John A. Magliacane, KD2BD, has held an Advanced Class license for over 31 years and a Commercial FCC Radio License since 1994. John holds Associate Degrees in Electronics Engineering Technology, Computer Science, and Mathematics/Physics, in addition to a Bachelor’s Degree in Electronics Engineering Technology.

John is employed at Brookdale Community College, Lincroft, NJ where he has served as a Learning Assistant in the Department of Engineering and Technology for over 27 years, as an advisor to the Brookdale Amateur

Radio Club since 1991, and as an Academic Tutor in the Computer Science Department. John has worked as a freelance technical writer for over 20 years, and authored weekly “SpaceNews” newsletters during the 1990s that gained world-wide popularity among the terrestrial packet radio networks and pacsat satellites that carried them.

John has been a Slackware Linux user for over 20 years, and has created and contributed to a number of open-source software projects. His “PREDICT” satellite tracking and “SPLAT!” RF propagation analysis applications have not only earned strong followings in the Amateur Radio and commercial telecommunications fields, but have also been adopted for use by scientists and engineers at NASA and the European Space Agency.

In addition to being a Frequency Measurement Test participant who employs receiving equipment and instrumentation entirely of his own design, John recently published the design of his “TriplePIC SSTV Video Scan Converter” that allows the exploration of vintage 8 second per frame monochrome slow-scan television using twenty first century electronics.

Notes

¹Michael A. Lombardi, Glenn K. Nelson, “WWVB: A Half Century of Delivering Accurate Frequency and Time by Radio,” *Journal of Research of the National Institute of Standards and Technology*, Volume 119, The National Institute of Standards and Technology, March 12, 2014.

²J. A. Adcock, VK3ACA, “Propagation of Long Radio Waves,” *Amateur Radio*, June to September 1991.

³Firmware for the PIC16F88 microcontroller is licensed under the GNU General Public License and is available for download from the ARRL QEX files website. Go to www.arrl.org/qexfiles and look for the file **11x15_Magliacane.zip**.

Additional References

“NIST Radio Station WWVB,” The National Institute of Standards and Technology, www.nist.gov/pml/div688/grp40/wwvb.cfm

“ARRL (and non-ARRL) Frequency Measuring Tests”, The American Radio Relay League, www.arrl.org/frequency-measuring-test/

John A. Magliacane, “KD2BD FMT Methodology,” www.qsl.net/kd2bd/fmt-methodology.html.